Interaction of excitons with a generalized Morse surface potential: *p*-polarization geometry of the incident light at a semiconductor surface

F. Pérez-Rodríguez and P. Halevi
Instituto de Física, Universidad Autónoma de Puebla, Apartado Postal J-48, 72570 Puebla, Puebla, México
(Received 20 September 1995)

We investigate theoretically the optical response of excitons localized near the surface of a semiconductor. Spectra of reflection of *p*-polarized light from strongly treated semiconductor surfaces are calculated by using a generalized Morse surface potential. The spectra exhibit prominent dips produced by the generation of exciton bound states and their corresponding longitudinal polariton modes. The position and the form of spectral dips depend not only on potential-well parameters but also on the value of the longitudinal-transverse splitting and the surface damping. Our results are compared with experimental spectra for CdSe and we also calculate reflectivity spectra for GaAs.

I. INTRODUCTION

In the past few years optical properties of excitons in confined systems have been intensively investigated.[1,2] Systems of this kind display interesting optical effects that frequently are not observed in crystals dominated by bulk behavior. The usual systems for confining excitons are thin films,[3–7] quantum wells,[8–11] quantum wires,[12–15] and quantum dots.[16–19] Nevertheless, excitons can also be confined in the vicinity of the surface of a semi-infinite semiconductor.[20,21] Indeed, surface treatments such as doping, electron and ion bombardment, application of electric field, and others, modify the concentration of impurity ions near the sample surface. The space charge produced gives rise to a macroscopic electric field and, as a result, to an extrinsic contribution to the excitonic surface potential. This contribution can be attractive, unlike intrinsic potentials, and can lead to the formation of a potential well. If the size of this well is sufficiently large, exciton bound states are generated. The optical manifestation of localized excitons within extrinsic surface potentials has been studied theoretically and experimentally.[22–36] However, several aspects of exciton confinement in surface-potential wells merit further study.

The generation of excitonic bound states leads to resonances in the optical spectra of reflectivity and transmission. The shape and position of these spectral resonances are determined by the form of the surface-potential well and by the coupling between localized excitons and light. In Refs. 24–32 the normal-incidence optical spectra were analyzed by employing a multiple-step model for the potential well. A more convenient, continuous model, based on the truncated Morse potential, was proposed in Refs. 33–36. The results obtained with these models show that in the case of *s*-polarized light excitonic bound states manifest themselves as maxima (minima) in the reflectivity (transmission). The positions of these extrema are close to exciton eigenfrequencies. They do not coincide exactly with the corresponding eigenvalues because of exciton-light coupling (polariton effect).

There is evidence of strong light-polarization dependence of the interaction between the electromagnetic field and confined excitons. Thus, for example, it was established that the shape of reflectivity spectra for quantum wells[11] and quantum well wires[13–15] drastically changes with switching from *s*-polarized light to *p*-polarized light. In the latter geometry, new spectral resonances (dips) appear. Recently,[35] we have reported a similar polarization effect in the reflectivity of semiconductors with near-surface localized excitons. Our calculations there gave rise to resonances (dips) that are manifestations of longitudinal, polarization waves. Among examples of the polarization effect, the experimental results of Ref. 37 should be mentioned too. In that work the changes in the spectra of reflection of *p*-polarized light from CdSe crystals, which had been subjected to distinct doses of electrons, were investigated. These changes turned out to be quite different from those obtained for normally incident light.

The aim of the present work is to investigate the interaction of excitons with strongly treated surfaces and the ensuing influence on the shape of optical spectra. This work is complementary to previous papers (Refs. 33, 34, and 36) and provides the full theoretical framework to another paper of ours.[35] Therefore, the theory is restricted here to the *p*-polarization geometry. We solve analytically the system of equations for the exciton-polariton fields using the generalized Morse surface potential (Sec. II). In Sec. III we employ our theory to interpret experimental reflectivity spectra[37] of CdSe (a II-VI semiconductor). Finally (Sec. IV), we analyze the peculiarities of the optical manifestation of near-surface localized excitons in III-V semiconductors.

II. THEORY

Let us assume that a nonlocal dielectric medium occupies the infinite half space $z>0$, with vacuum in the region $z<0$. At the dielectric surface ($z=0$), *p*-polarized light is incident with an electric field

$$\mathbf{E}_i(x,z,t)=E_i[1,0,-q_x/q_z]e^{iq_x x+iq_z z-i\omega t}, \tag{1}$$

where q_x, q_z are the components of the wave vector,

$$q_x=q\sin\theta, \quad q_z=q\cos\theta, \quad q=\omega/c, \tag{2}$$

θ is the angle of incidence, ω is the circular frequency, and c is the speed of light in vacuum. The reflected field has the form

$$\mathbf{E}_r(x,z,t)=E_r[1,0,q_x/q_z]e^{iq_x x-iq_z z-i\omega t}. \tag{3}$$

Inside the dielectric medium ($z>0$) the electric field $\mathbf{E}$ satisfies the Maxwell equations, which are coupled to the equation of motion for the excitonic polarization $\mathbf{P}$.[21] The system of coupled equations is written as follows:

$$\left(\frac{\partial^2}{\partial z^2}+\Gamma^2(z)\right)\mathbf{P}=-\frac{\omega_P^2 M}{4\pi\hbar\omega_T}\mathbf{E},$$

$$\nabla\times\nabla\times\mathbf{E}-\epsilon_\infty q^2\mathbf{E}=4\pi q^2\mathbf{P}, \tag{4}$$

where

$$\Gamma^2(z)=\Gamma_B^2+\Delta\Gamma^2(z),$$

$$\Gamma_B^2=\frac{M}{\hbar\omega_T}\left[\omega^2-\omega_T^2-\frac{\hbar\omega_T}{M}q_x^2+i\omega\nu\right],$$

$$\Delta\Gamma^2(z)=-\frac{2MU(z)}{\hbar^2}. \tag{5}$$

Here M is the exciton mass, ω_T is the frequency of the exciton resonance, ω_P is a measure of the oscillator strength, ϵ_∞ is the high-frequency (background) dielectric constant, and ν is the damping constant. The surface potential $U(z)$ appears in the formula for $\Gamma^2(z)$ (5) and is modeled by means of the generalized Morse surface potential,

$$U(z)=\begin{cases} U_1e^{-z/a}+U_2e^{-2z/a}, & z>0 \\ \infty, & z<0. \end{cases} \tag{6}$$

According to the assumed geometry of p polarization, the exciton-polariton fields in an isotropic medium can be expressed as

$$\mathbf{E}(x,z,t)=[E_x(z),0,E_z(z)]e^{iq_x x-i\omega t},$$
$$\mathbf{P}(x,z,t)=[P_x(z),0,P_z(z)]e^{iq_x x-i\omega t}. \tag{7}$$

Hence the system (4) takes the form

$$\left(\frac{\partial^2}{\partial z^2}+\Gamma^2(z)\right)P_x(z)=-\frac{\omega_P^2 M}{4\pi\hbar\omega_T}E_x(z),$$

$$\left(\frac{\partial^2}{\partial z^2}+\Gamma^2(z)\right)P_z(z)=-\frac{\omega_P^2 M}{4\pi\hbar\omega_T}E_z(z), \tag{8}$$

$$iq_x\frac{\partial E_z(z)}{\partial z}-\left(\frac{\partial^2}{\partial z^2}+\epsilon_\infty q^2\right)E_x(z)-4\pi q^2P_x(z)=0,$$

$$iq_x\frac{\partial E_x(z)}{\partial z}+(q_x^2-\epsilon_\infty q^2)E_z(z)-4\pi q^2P_z(z)=0. \tag{9}$$

After eliminating the x and z components of the electric field from the system of Eqs. (8) and (9), we obtain two coupled equations for the components of the excitonic polarization, which can be written as follows:

$$\left[\frac{\partial^2}{\partial z^2}+\epsilon_\infty q^2-q_x^2\right]\left\{\left[\frac{\partial^2}{\partial z^2}+\Gamma_B^2+\Delta\Gamma^2(z)\right]P_x(z)\right\}$$
$$-\frac{\omega_p^2 M}{\epsilon_\infty\hbar\omega_T}(\epsilon_\infty q^2-q_x^2)P_x(z)-iq_x\frac{\omega_p^2 M}{\epsilon_\infty\hbar\omega_T}\frac{\partial P_z(z)}{\partial z}=0,$$

$$iq_x\frac{\partial}{\partial z}\left\{\left[\frac{\partial^2}{\partial z^2}+\Gamma_B^2+\Delta\Gamma^2(z)\right]P_x(z)\right\}+q^2\frac{\omega_p^2 M}{\hbar\omega_T}P_z(z)$$
$$-(\epsilon_\infty q^2-q_x^2)\left[\frac{\partial^2}{\partial z^2}+\Gamma_B^2+\Delta\Gamma^2(z)\right]P_z(z)=0. \tag{10}$$

In a semispace ($z>0$) the functions $P_x(z)$, $P_z(z)$ can be expressed as a linear combination of three independent solutions of (10). Thus,

$$P_x(z)=\sum_{s=1}^{3}P_x^{(s)}(z),\quad P_x^{(s)}(z)=e^{iq_s z}F_s(z);$$

$$P_z(z)=\sum_{s=1}^{3}P_z^{(s)}(z),\quad P_z^{(s)}(z)=e^{iq_s z}G_s(z). \tag{11}$$

Here q_s ($s=1,2,3$; $\mathrm{Im}q_s>0$) are z components of the wave vector for modes propagating towards the bulk, where $\Delta\Gamma^2(z)\to 0$ and the functions $F_s(z)$, $G_s(z)$ are, in fact, constants. The values q_1 and q_2 are the z components of the transverse modes and are given by the formula

$$q_{1,2}=\left\{\frac{1}{2}\left[\Gamma_B^2+\epsilon_\infty q^2-q_x^2\pm\left([\Gamma_B^2-\epsilon_\infty q^2+q_x^2]^2+\frac{4\omega_P^2\omega^2 M}{c^2\hbar\omega_T}\right)^{1/2}\right]\right\}^{1/2}. \tag{12}$$

The value q_3 is the z component of the longitudinal mode and is expressed as

$$q_3=\left(\Gamma_B^2-\frac{\omega_P^2 M}{\epsilon_\infty\hbar\omega_T}\right)^{1/2}. \tag{13}$$

Near the surface ($z\leqslant a$, where a is the characteristic width of the excitonic surface potential) the behavior of the excitonic polarization $\mathbf{P}$ (11) is determined by the functions $F_s(z)$, $G_s(z)$. In the case of the generalized Morse surface potential [Eq. (6)] these functions have the form (see Appendix)

$$F_s(z)=\sum_{k=0}^{\infty}a_{ks}e^{-kz/a},\quad G_s(z)=\sum_{k=0}^{\infty}b_{ks}e^{-kz/a}. \tag{14}$$

The recursion relations for the coefficients a_{ks}, b_{ks} ($s=1,2,3$) of series (14) are given by Eqs. (A10)–(A13). Because these relations are coupled there are only three independent coefficients. Without loss of generality, we can choose $a_{0,1}$, $a_{0,2}$, and $b_{0,3}$ to be the independent coefficients.

The expression for the electric field $\mathbf{E}$ (7) is obtained by using (8) and (11). We find

$$E_x(z)=-\frac{4\pi\hbar\omega_T}{\omega_P^2 M}\sum_{s=1}^{3} e^{iq_s z}\left[\frac{\partial^2 F_s}{\partial z^2}+2iq_s\frac{\partial F_s}{\partial z}+[\Gamma^2(z)-q_s^2]F_s(z)\right],$$

$$E_z(z)=-\frac{4\pi\hbar\omega_T}{\omega_P^2 M}\sum_{s=1}^{3} e^{iq_s z}\left[\frac{\partial^2 G_s}{\partial z^2}+2iq_s\frac{\partial G_s}{\partial z}+[\Gamma^2(z)-q_s^2]G_s(z)\right]. \quad (15)$$

The coefficientes $a_{0,1}$, $a_{0,2}$, and $b_{0,3}$ in Eq. (14) and the amplitude E_r in Eq. (3) should be found from the boundary conditions. We will apply the continuity conditions on the tangential components of the electric and magnetic fields at the surface $z=0$ and the ''additional boundary condition'' for the excitonic polarization,[33]

$$\mathbf{P}(z=0)=0. \quad (16)$$

After calculating E_r, we get straightforwardly the reflectivity $R=|E_r/E_i|^2$.

The formalism developed above allows us to calculate the reflectivity spectra for semiconductors with a surface-potential well. As was mentioned in the Introduction, the generation of bound states in the potential well may produce resonances in the optical spectra. These states of excitons localized near the surface are found from the Schrödinger equation for the translational motion,[21]

$$\frac{\hbar^2}{2M}\left(q_x^2-\frac{\partial^2}{\partial z^2}\right)\psi(z)+[\hbar\omega_T+U(z)]\psi(z)=\hbar\omega\psi(z), \quad (17)$$

with the boundary conditions

$$\psi(0)=0, \quad \psi(\infty)=0. \quad (18)$$

The quantity q_x in (17) coincides with the x component of the wave vector of the incident light [Eq. (2)]. So, the eigenvalues of energy $\hbar\omega_{Tn}$ for the potential well $\hbar\omega_T+U(z)$ can be expressed in the form

$$\hbar\omega_{Tn}=\hbar\omega_{Tn}^{(0)}+\frac{\hbar^2 q_x^2}{2M}, \quad (19)$$

where $\hbar\omega_{Tn}^{(0)}$ are the eigenenergies for the case of normal incidence of light. They are calculated numerically. The second term on the right-hand side of Eq. (19) gives a small contribution to the eigenvalues, which is of the order of 10^{-5} eV.

The eigenstates manifest themselves in the reflectivity spectra as prominent maxima (broad peaks) whose positions are near their corresponding eigenfrequency. However, as the incidence angle θ is increased, new resonance structures may appear.[35] This is a polarization effect since the new resonances (dips) are absent in the case of s-polarization geometry (Refs. 33 and 34). The appearance of spectrum dips at frequencies that differ notably from eigenvalues of exciton bound states can be explained by means of the following analysis.

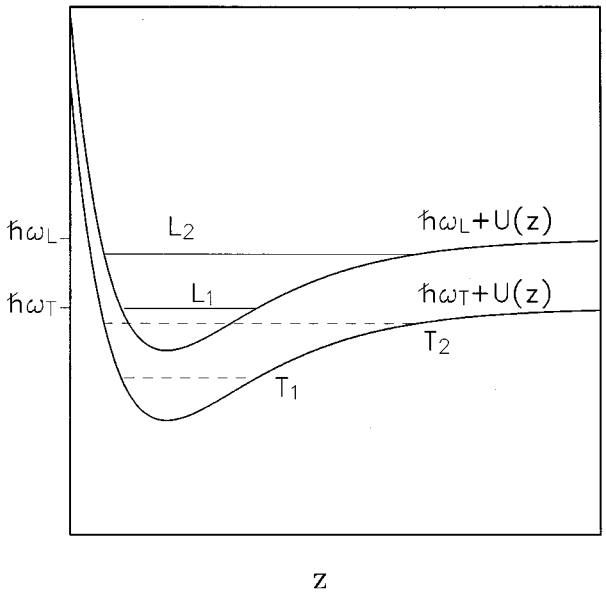

FIG. 1. Mechanical, $\hbar\omega_T+U(z)$, and ''longitudinal,'' $\hbar\omega_L+U(z)$, exciton potentials with bound states.

In spatially dispersive media, longitudinal normal modes are excited in the p-polarization geometry. As a consequence, the component of the electric field, which is perpendicular to the surface, can couple strongly to quasiparticles in the crystal.[21] The condition for exciting longitudinal normal modes is the vanishing of the displacement vector,

$$\mathbf{D}=\epsilon_\infty\mathbf{E}+4\pi\mathbf{P}. \quad (20)$$

Under this condition ($\mathbf{D}=0$) the first equation in (4) can be rewritten in terms exclusively of the excitonic polarization:

$$\frac{\hbar^2}{2M}\left(q_x^2-\frac{\partial^2}{\partial z^2}\right)\mathbf{P}+[\hbar\omega_L+U(z)]\mathbf{P}=\hbar\omega\mathbf{P}, \quad (21)$$

where ω_L is the exciton longitudinal frequency,

$$\omega_L\approx\omega_T+\frac{\omega_P^2}{2\omega_T\epsilon_\infty}. \quad (22)$$

In obtaining Eq. (21) we omitted the damping term and we took into account that the differences between ω, ω_T, and ω_L are very small. Obviously, Eq. (21) is also satisfied by the electric field $\mathbf{E}$.

Notice Eq. (21) is the one-dimensional Schrödinger equation for the mechanical exciton [Eq. (17)], with the wave function $\psi(z)$ and the mechanical potential $\hbar\omega_T+U(z)$ replaced by the excitonic polarization $\mathbf{P}$ and the ''longitudinal'' exciton potential $\hbar\omega_L+U(z)$, respectively. Hence, the eigenvalues $\hbar\omega_{Ln}$ of the polarization wave $\mathbf{P}$ are simply shifted (Fig. 1), in comparison to exciton bound states ($\hbar\omega_{Tn}$), by the longitudinal-transverse splitting $\hbar\omega_{\mathrm{LT}}\equiv\hbar\omega_L-\hbar\omega_T$ [Eq. (23)]. These quantized polarization modes give rise to resonant dips at frequencies ω_{Ln} in the reflectivity.[35] According to Eq. (19), eigenfrequencies $\omega_{Ln}=\omega_{Tn}+\omega_{\mathrm{LT}}$ depend on incidence angle θ.

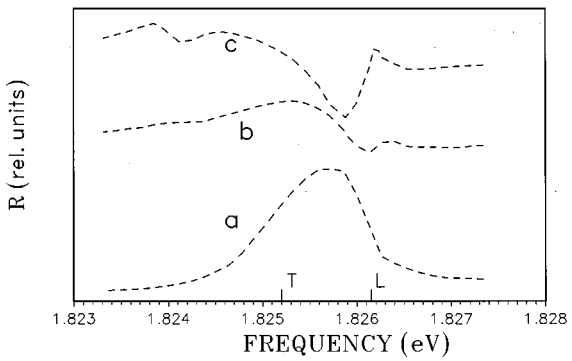

FIG. 2. Experimental reflection spectra of CdSe obtained in Ref. 37 by Batyrev, Karasenko, and Sel'kin for p-polarized light ($\theta=83°$) and different durations of electron bombardment: (a) initial state (before bombardment); after bombardment with (b) 3.5-keV electrons for 9.5 min, and (c) 4.5-keV electrons for 22 min.

Below we shall use the present theory to interpret experimental results and analyze the manifestation of near-surface localized excitons in both II-VI and III-V semiconductors.

III. COMPARISON WITH EXPERIMENT (CdSe)

Spectra of oblique reflection of light from strongly treated CdSe crystals were experimentally investigated in Ref. 37. The surface transition layers were produced by bombarding the samples with electrons of a few keV. In Fig. 2 we present reflection spectra obtained in Ref. 37 for oblique incidence ($\theta=83°$) of light and different durations of electron irradiation: (a) initial state (before irradiation); after irradiation with 3.5-keV electrons for 9.5 min (b), and with 4.5-keV electrons for 22 min (c). From Fig. 2 it is clear that optical spectra undergo notable changes due to the surface treatment. In order to interpret these experimental results we calculated the CdSe reflection spectra (Fig. 3) using different surface potentials $U(z)$ [Eq. (6)]; exponential [Fig. 4(a)]:

$$U(z)=U_1e^{-z/a}, \tag{23}$$

with $U_1=1$ meV, $a=60$ Å; and two potential wells of different sizes having the form of the ''classical'' Morse petential, truncated at $z=0$ [Figs. 4(b,c)],

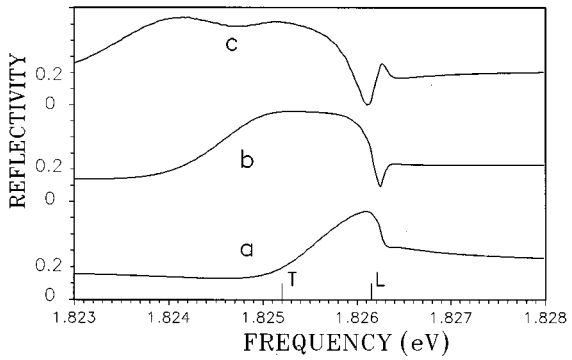

FIG. 3. Reflectivity spectra of CdSe for p-polarized light ($\theta=83°$). The curves (a), (b), and (c) were calculated with the respective surface potentials (a), (b), and (c), shown in Fig. 4.

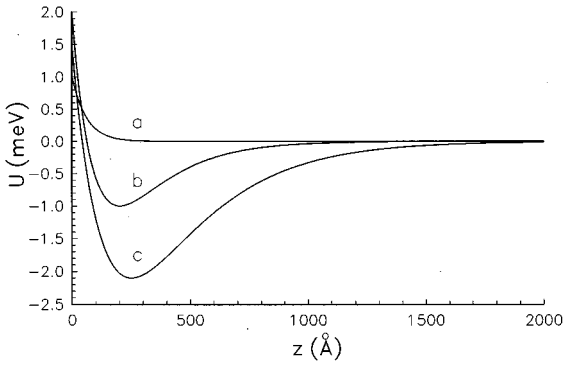

FIG. 4. Graphs of the surface potentials $U(z)$: (a) exponential (intrinsic), $U_1=1$ meV, $U_2=0$, $a=60$ Å; (b) well, $U_m=-1$ meV, $a=200$ Å, $z_m=200$ Å; (c) well, $U_m=-2.1$ meV, $a=300$ Å, $z_m=250$ Å.

$$\mathrm{Re}U(z)=|U_m|[e^{-2(z-z_m)/a}-2e^{-(z-z_m)/a}],$$

$$\mathrm{Im}U(z)=\mathrm{Im}U_1e^{-z/a}, \tag{24}$$

that is,

$$\mathrm{Re}U_1=-2|U_m|e^{z_m/a},\quad \mathrm{Re}U_2=|U_m|e^{2z_m/a}. \tag{25}$$

Here z_m denotes the position of the surface-potential minimum [$U(z_m)=U_m$]. The respective parameters used are $U_m=-1$ meV, $a=z_m=200$ Å, $\mathrm{Im}U_1=-0.6$ meV, $\mathrm{Im}U_2=0$ [Fig. 4(b)]; and $U_m=-2.1$ meV, $a=300$ Å, $z_m=250$ Å, $\mathrm{Im}U_1=-0.6$ meV, $\mathrm{Im}U_2=0$ [Fig. 4(c)]. Other parameters are $\hbar\omega_T=1.825\,20$ eV, $\hbar\omega_P=0.1715$ eV ($\hbar\omega_L=1.826\,15$ eV), $\epsilon_\infty=8.4$, $\nu=0.1$ meV, $M=0.415m$ (m is the free-electron mass). The well (c) is both wider and deeper than the well (b).

The reflection curves (Fig. 3) for the chosen surface potentials reproduce qualitatively the experimental spectra. So, when the size of the surface-potential well is increased [from (b) to (c)], the reflection line shape changes notably. We shall demonstrate that this structure may be produced by the generation of excitonic bound states near the surface, however strongly attenuated by surface (rather than bulk) damping.

The potential well (b) has two ($n_b=1,2$) excitonic bound states at

$$\hbar\omega_{T1}^{(b)}=1.824\,65\ \text{eV},\quad \hbar\omega_{T2}^{(b)}=1.825\,14\ \text{eV}, \tag{26}$$

and the well (c) has four eigenstates ($n_c=1,2,3,4$) at

$$\hbar\omega_{T1}^{(c)}=1.823\,55\ \text{eV},\quad \hbar\omega_{T2}^{(c)}=1.824\,29\ \text{eV},$$

$$\hbar\omega_{T3}^{(c)}=1.824\,81\ \text{eV},\quad \hbar\omega_{T4}^{(c)}=1.825\,11\ \text{eV}. \tag{27}$$

The transverse resonances, which of course are also present in the s-polarization geometry,[33] have the form of broad peaks below ω_T and near ω_{Tn} (see solid lines in Figs. 5 and 6). In addition, the generation of quantized polarization waves gives rise to resonant dips that are close to ω_{Ln}. Unfortunately, the identification of peaks and dips with the nominal ω_{Tn}'s and ω_{Ln}'s is not easy. However, because of the increase in damping in the extrinsic transition layer[30,31] [$\Delta\nu(z)=-2\mathrm{Im}U(z)/\hbar$], all resonances are smoothed out and two or more of them may coalesce into a single one

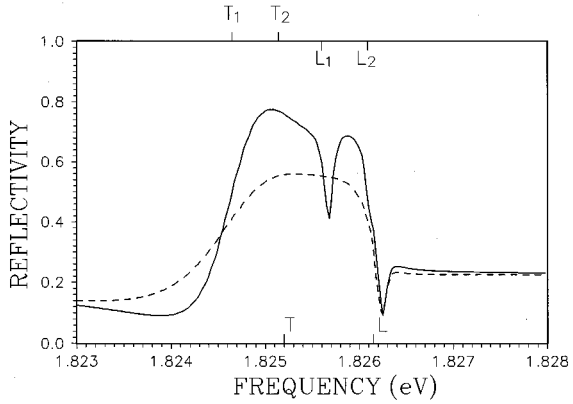

FIG. 5. Reflectivity spectrum of CdSe for p-polarized light with angle of incidence $\theta=83°$. The parameters of the surface-potential well are the same as in Fig. 3(b), and the dashed curve is the same as Fig. 3(b). The surface damping is $\Delta\nu(0)=0$ (solid line), $\Delta\nu(0)=1.2$ meV (dashed curve).

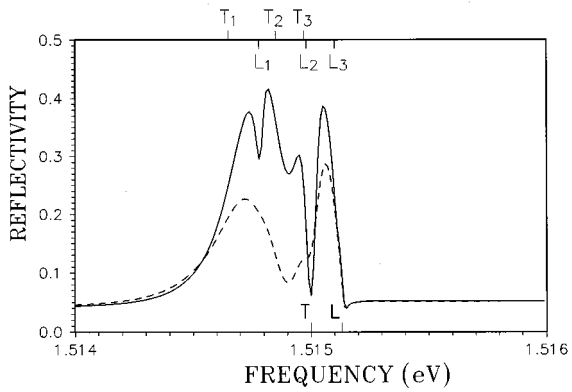

FIG. 7. Reflectivity spectrum of GaAs for p-polarized light with angle of incidence $\theta=80°$. The parameters of the surface-potential well are $U_m=-0.5$ meV, $a=550$ Å, $z_m=550$ Å. The surface damping is $\Delta\nu(0)=0$ (solid line), $\Delta\nu(0)=0.1$ meV (dashed curve).

(dashed lines in Figs. 5 and 6). The process of formation of the reflection line shape, as surface damping is increased, can be observed in Figs. 5 and 6 [the dashed lines are the same as Figs. 3(b,c)]. This allows us to conlcude that the peaks and dips observed in the experiment (Fig. 2) are likely to be caused by transverse and longitudinal resonances, respectively, whose structure depends considerably on surface damping.

IV. SMALL LONGITUDINAL-TRANSVERSE SPLITTING (GaAs)

Besides the surface damping, there is another factor that also affects the structure of spectral resonances. It is associated with the value of the longitudinal-transverse splitting. When $\hbar\omega_{\mathrm{LT}}$ is small in comparison with the depth $|U_m|$ of the surface-potential well, the longitudinal resonances (ω_{Ln}) may appear below ω_T. This means that longitudinal and transverse resonances will interfere, as can happen even for group II-VI semiconductors (see Fig. 6). In particular, this fact concerns semiconductors of the group III-V because of their relatively small longitudinal-transverse splitting.[21] In this case the ''polariton effect'' on the resonances is considerable.

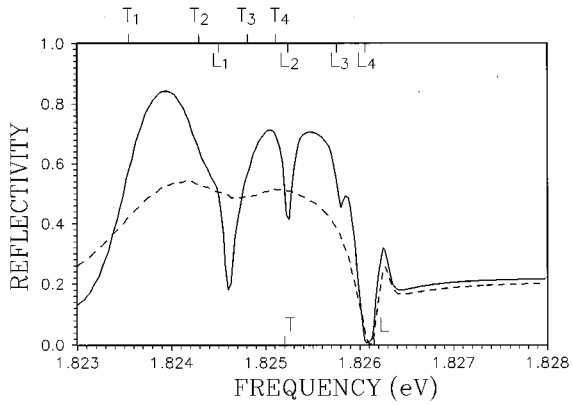

FIG. 6. Refectivity spectrum of CdSe for p-polarized light with angle of incidence $\theta=83°$. The parameters of the surface-potential well are the same as in Fig. 3(c), and the dashed curve is the same as Fig. 3(c). The surface damping is $\Delta\nu(0)=0$ (solid line), $\Delta\nu(0)=1.2$ meV (dashed curve).

In Fig. 7 the p-polarization reflectivity spectrum of a III-V semiconductor (GaAs) is shown. The spectrum was calculated for the incidence angle $\theta=80°$. The parameters used for the GaAs crystal are[38] $\hbar\omega_T=1.515$ eV, $\hbar\omega_P=0.071\,06$ eV, $\hbar\nu=0.035$ meV, $\epsilon_\infty=12.6$. Here we applied the approximation of a single exciton branch with an average mass $M=0.298m$.[39] We employed a potential well as in Eq. (24) with parameters $U_m=-0.5$ meV, $a=550$ Å, $z_m=550$ Å. For this potential well there are three excitonic bound states:

$$\hbar\omega_{T1}=1.514\,65\ \text{eV},\quad \hbar\omega_{T2}=1.514\,85\ \text{eV},$$

$$\hbar\omega_{T3}=1.514\,97\ \text{eV}. \tag{28}$$

The corresponding longitudinal eigenvalues $\hbar\omega_{Ln}$ ($n=1,2,3$) are shifted by the longitudinal-transverse splitting $\hbar\omega_{\mathrm{LT}}=0.13$ meV, which is approximately four times smaller than the well depth $|U_m|$. In Fig. 7 various peaks and dips are observed near the transverse and longitudinal eigenvalues when the surface damping $\Delta\nu(x)=0$. Note that the resonances $L2$ and $T3$ are practically at the same frequency and, as a consequence, they interfere. After increasing the surface damping the reflection spectrum changes radically (see Fig. 7). There, it can be seen that the wide dip below $\hbar\omega_T$ in the reflection spectrum is a result of the generation of the longitudinal modes $L1$ and $L2$.

It should be noted that the excitonic reflection spectra of GaAs crystals with treated surfaces have been investigated in various works.[25,33,40–42] The spectra of reflection of light with polarization parallel to the plane of incidence were analyzed in Ref. 42. There it was shown that the application of an electric field affects notably the excitonic spectra. The surface-potential wells, which were produced by the applied electric fields, were of relatively small depths and the surface damping was considerable. For this reason, after increasing

the electric field at the sample surface, the appearance of only one new dip in the oblique-incidence reflection spectrum below ω_L was observed.

V. CONCLUSION

The developed theory allows us to explain qualitatively the changes in the reflectivity spectra for p polarization that are observed in semiconductors with strongly treated surfaces. The changes are due to the generation of excitonic bound states. In this geometry the near-surface localized excitons produce transverse (broad peaks) and longitudinal (dips) resonances in the reflectivity spectra. The number and form of the dips are considerably affected not only by the parameters of the surface-potential well, but also by the value of the longitudinal-transverse splitting ω_{LT} and the surface damping $\Delta\nu(z)$. These results should be useful for determining the profile of the surface-potential well. However, in order to obtain trustworthy models $U(z)$ it would be necessary to compare with miscellaneous experimental spectra (s- and p-polarized reflectivity, attenuated total reflection, etc.) of the same sample.

ACKNOWLEDGMENTS

We are grateful to A.V. Sel'kin and B. Flores-Desirena for stimulating discussions. This work was partially supported by the Consejo Nacional de Ciencia y Tecnología (CONACyT) under Grant No. 3923 E 9402.

APPENDIX: RECURSION RELATIONS

Substituting the expressions (11) for $P_x(z)$, $P_z(z)$ into Eqs. (10), we obtain a system of equations for the functions $F_s(z)$, $G_s(z)$ $(s=1,2,3)$:

$$\frac{\partial^4 F_s}{\partial z^4}+4iq_s\frac{\partial^3 F_s}{\partial z^3}+[-6q_s^2+\Gamma_B^2+\epsilon_\infty q^2-q_x^2+\Delta\Gamma^2(z)]\frac{\partial^2 F_s}{\partial z^2}+\left[-4iq_s^3+2iq_s(\Gamma_B^2+\epsilon_\infty q^2-q_x^2)+2iq_s\Delta\Gamma^2(z)+2\frac{\partial\Delta\Gamma^2}{\partial z}\right]\frac{\partial F_s}{\partial z}+\left[q_s^4-q_s^2(\Gamma_B^2+\epsilon_\infty q^2-q_x^2)+\Gamma_B^2(\epsilon_\infty q^2-q_x^2)-\frac{\omega_P^2 M}{\epsilon_\infty\hbar\omega_T}(\epsilon_\infty q^2-q_x^2)+(-q_s^2+\epsilon_\infty q^2-q_x^2)\Delta\Gamma^2(z)+2iq_s\frac{\partial\Delta\Gamma^2}{\partial z}+\frac{\partial^2\Delta\Gamma^2}{\partial z^2}\right]F_s(z)-iq_x\frac{\omega_P^2 M}{\epsilon_\infty\hbar\omega_T}\left[iq_sG_s(z)+\frac{\partial G_s}{\partial z}\right]=0. \tag{A1}$$

$$iq_x\left[\frac{\partial^3 F_s}{\partial z^3}+3iq_s\frac{\partial^2 F_s}{\partial z^2}+[-3q_s^2+\Gamma_B^2+\Delta\Gamma^2(z)]\frac{\partial F_s}{\partial z}+\left(-iq_s^3+iq_s\Gamma_B^2+iq_s\Delta\Gamma^2(z)+\frac{\partial\Delta\Gamma^2}{\partial z}\right)F_s(z)\right]-(\epsilon_\infty q^2-q_x^2)\left[\frac{\partial^2 G_s}{\partial z^2}+2iq_s\frac{\partial G_s}{\partial z}\left(-q_s^2+\Gamma_B^2+\Delta\Gamma^2(z)-\frac{\omega_P^2 M}{\hbar\omega_T}\frac{q^2}{\epsilon_\infty q^2-q_x^2}\right)G_s(z)\right]=0, \tag{A2}$$

To solve this system of equations with the surface potential $U(z)$ [Eq. (6)], it is convenient to introduce the variable

$$\zeta=e^{-z/a}. \tag{A3}$$

We obtain

$$\zeta^4\frac{\partial^4 f_s}{\partial\zeta^4}+\alpha_{1s}\zeta^3\frac{\partial^3 f_s}{\partial\zeta^3}+[\alpha_{2s}\zeta^2+\alpha_{3s}\zeta^3+\alpha_{4s}\zeta^4]\frac{\partial^2 f_s}{\partial\zeta^2}+[\alpha_{5s}\zeta+\alpha_{6s}\zeta^2+\alpha_{7s}\zeta^3]\frac{\partial f_s}{\partial\zeta}+[\alpha_{10s}+\alpha_{8s}\zeta+\alpha_{9s}\zeta^2]f_s+\alpha_{11s}\zeta\frac{\partial g_s}{\partial\zeta}+\alpha_{12s}g_s=0, \tag{A4}$$

$$\alpha_{13s}\zeta^3\frac{\partial^3 f_s}{\partial\zeta^3}+\alpha_{14s}\zeta^2\frac{\partial^2 f_s}{\partial\zeta^2}+[\alpha_{15s}\zeta+\alpha_{16s}\zeta^2+\alpha_{17s}\zeta^3]\frac{\partial f_s}{\partial\zeta}+[\alpha_{18s}+\alpha_{19s}\zeta+\alpha_{20s}\zeta^2]f_s+\alpha_{21s}\zeta^2\frac{\partial^2 g_s}{\partial\zeta^2}+\alpha_{22s}\zeta\frac{\partial g_s}{\partial\zeta}+[\alpha_{23s}+\alpha_{24s}\zeta+\alpha_{25s}\zeta^2]g_s=0. \tag{A5}$$

Here the functions $f_s(\zeta)$ $(s=1,2,3)$ are defined by

$$f_s=(\zeta(z))=F_s,\quad g_s(\zeta(z))=G_s(z). \tag{A6}$$

The coefficients α_{is} $(i=1,2,\ldots,9;\ s=1,2,3)$ have the same form as in Eqs. (18) of our previous paper, Ref. 33 (even for $s=3$). Other coefficients are

$$\alpha_{10s}=\frac{\omega_P^2 M}{\epsilon_\infty \hbar \omega_T} q_x^2 a^4+\left(\Gamma_B^2(\epsilon_\infty q^2-q_x^2)-\frac{q^2\omega_P^2 M}{\hbar\omega_T}\right)a^4+(\Gamma_B^2+\epsilon_\infty q^2-q_x^2)a^2\kappa_s^2+\kappa_s^4, \quad \alpha_{11s}=iq_x a^3\frac{\omega_P^2 M}{\epsilon_\infty\hbar\omega_T},$$

$$\alpha_{12s}=-iq_x a^3\kappa_s\frac{\omega_P^2 M}{\epsilon_\infty\hbar\omega_T}, \quad \alpha_{13s}=-q_x a, \quad \alpha_{14s}=iq_s a(3\kappa_s-3),\ \alpha_{15s}=-iq_x a(3\kappa_s^2+\Gamma_B^2 a^2-3\kappa_s+1), \quad \alpha_{16s}=iq_x a\frac{U_1}{W},$$

$$\alpha_{17s}=iq_x a\frac{U_2}{W}, \quad \alpha_{18s}=iq_x a(\kappa_s^3+\Gamma_B^2 a^2\kappa_s), \quad \alpha_{19s}=iq_x a(1-\kappa_s)\frac{U_1}{W}, \quad \alpha_{20s}=iq_x a(2-\kappa_s)\frac{U_2}{W}, \quad \alpha_{21s}=-a^2(\epsilon_\infty q^2-q_x^2),$$

$$\alpha_{22s}=-a^2(\epsilon_\infty q^2-q_x^2)(1-2\kappa_s), \quad \alpha_{23s}=-a^2(\epsilon_\infty q^2-q_x^2)\left(\kappa_s^2+\Gamma_B^2 a^2-\frac{\omega_P^2 M}{\hbar\omega_T}\frac{q^2a^2}{\epsilon_\infty q^2-q_x^2}\right),$$

$$\alpha_{24s}=a^2(\epsilon_\infty q^2-q_x^2)\frac{U_1}{W}, \quad \alpha_{25s}=a^2(\epsilon_\infty q^2-q_x^2)\frac{U_2}{W}. \tag{A7}$$

The quantities κ_s and W are expressed as

$$\kappa_s=iq_s a, \quad W=\hbar^2/2a^2M. \tag{A8}$$

The coupled equations (A4),(A5) can be solved by writing

$$f_s(\zeta)=\sum_{k=0}^{\infty} a_{ks}\zeta^k; \quad g_s(\zeta)=\sum_{k=0}^{\infty} b_{ks}\zeta^k. \tag{A9}$$

Substituting Eq. (A9) into Eqs. (A4),(A5), we obtain a system of recursion relations for a_{ks} and b_{ks} ($s=1,2,3$) with $k\geqslant 2$:

$$\begin{aligned}&a_{ks}[k(k-1)(k-2)(k-3)+\alpha_{1s}k(k-1)(k-2)+\alpha_{2s}k(k-1)+\alpha_{5s}k+\alpha_{10s}]+a_{k-1,s}[\alpha_{3s}(k-1)(k-2)+\alpha_{6s}(k-1)+\alpha_{8s}]\\&\quad+a_{k-2,s}[\alpha_{4s}(k-2)(k-3)+\alpha_{7s}(k-2)+\alpha_{9s}]+b_{ks}[\alpha 11sk+\alpha_{12s}]=0,\\&a_{ks}[\alpha_{13s}k(k-1)(k-2)+\alpha_{14s}k(k-1)+\alpha_{15s}k+\alpha 18s]+a_{k-1,s}[\alpha_{16s}(k-1)+\alpha_{19s}]+a_{k-2,s}[\alpha_{17s}(k-2)+\alpha_{20s}]\\&\quad+b_{ks}[\alpha_{21s}k(k-1)+\alpha_{22s}k+\alpha_{23s}]+b_{k-1,s}\alpha_{24s}+b_{k-2,s}\alpha_{25s}=0.\end{aligned} \tag{A10}$$

The terms a_{1s} and b_{1s} are obtained from the system of equations

$$\begin{aligned}&a_{1s}[\alpha_{5s}+\alpha_{10s}]+b_{1s}[\alpha_{12s}+\alpha_{11s}]=-a_{0s}\alpha_{8s},\\&a_{1s}[\alpha_{15s}+\alpha_{18s}]+b_{1s}[\alpha_{22s}+\alpha_{23s}]=-a_{0s}\alpha_{19s}-b_{0s}\alpha_{24s},\end{aligned} \tag{A11}$$

where

$$b_{0s}=-\frac{\alpha_{10s}}{\alpha_{12s}}a_{0s} \quad \text{for } s=1,2 \tag{A12}$$

and

$$a_{0s}=-\frac{\alpha_{12s}}{\alpha_{10s}}b_{0s} \quad \text{for } s=3. \tag{A13}$$

So, there are only three independent coefficients ($a_{0,1}$, $a_{0,2}$, and $b_{0,3}$) that are found from boundary conditions.

[1] *Excitons in Confined Systems*, edited by R. Del Sole, A. D'Andrea, and A. Lapiccirella, Springer Proceedings in Physics Vol. 25 (Springer, Berlin, 1987), and references therein.
[2] L.C. Andreani, in *Confined Electrons and Photons: New Physics and Devices*, edited by E. Burstein and C. Weisbuch (Plenum Press, New York, 1994), and references therein.
[3] K. Cho, A. D'Andrea, R. Del Sole, and H. Ishihara, J. Phys. Soc. Jpn. **59**, 1853 (1990).
[4] A. D'Andrea and R. Del Sole, Phys. Rev. B **41**, 1413 (1990).
[5] H. Ishihara and K. Cho, Phys. Rev. B **41**, 1424 (1990).
[6] Y. Chen, F. Bassani, J. Massies, C. Deparis, and G. Neu, Europhys. Lett. **14**, 483 (1991).
[7] A. Tredicucci, Y. Chen, F. Bassani, J. Massies, C. Deparis, and G. Neu, Phys. Rev. B **47**, 10 348 (1993).
[8] L. Schultheis and K. Ploog, Phys. Rev. B **30**, 1090 (1984).
[9] E.I. Ivchenko, V.P. Kochereshko, P.S. Kop'ev, V.A. Kosobukin, I.N. Uraltsev, and D.R. Yakovlev, Solid State Commun. **70**, 529 (1989).
[10] B. Deveaud, F. Clérot, N. Roy, K. Satzke, B. Sermage, and D.S. Katzer, Phys. Rev. Lett. **67**, 2355 (1991).
[11] F. Tassone, F. Bassani, and L.C. Andreani, Phys. Rev. B **45**, 6023 (1992).
[12] U. Bockelmann and G. Bastard, Europhys. Lett. **15**, 215 (1991).
[13] M. Kohl, D. Heitmann, P. Grambow, and K. Ploog, Phys. Rev. B **37**, 10 927 (1988).
[14] M. Kohl, D. Heitmann, P. Grambow, and K. Ploog, Phys. Rev. B **42**, 2941 (1990).
[15] A. D'Andrea and R. Del Sole, Phys. Rev. B **46**, 2363 (1992).
[16] W. Que, Solid State Commun. **81**, 721 (1992).
[17] W. Que, Phys. Rev. B **45**, 11 036 (1992).
[18] G.T. Einevoll, Phys. Rev. B **47**, 3410 (1992).
[19] S.I. Pokutnyi, Phys. Lett. A **168**, 433 (1992).
[20] A.E. Cherednichenko and V.A. Kiselev, Prog. Surf. Sci. **36**, 177 (1991).
[21] P. Halevi, in *Spatial Dispersion in Solids and Plasmas*, edited by P. Halevi, Electromagnetic Waves–Recent Developments in Research Vol. 1 (Elsevier, Amsterdam, 1992), Chap. 6.
[22] V.A. Zuev, D.V. Korbutyak, M.V. Kurik, V.G. Litovchenko, A. Kh. Rozhko, and P.A. Skubneko, Pis'ma Zh. Éksp. Teor. Fiz. **26**, 455 (1977) [JETP Lett. **26**, 327 (1977)].
[23] V.A. Kiselev, Fiz. Tverd. Tela (Leningrad) **20**, 1191 (1978) [Sov. Phys. Solid State **20**, 685 (1978)].
[24] V.A. Kiselev, Fiz. Tverd. Tela (Leningrad) **20**, 2173 (1978) [Sov. Phys. Solid State **20**, 1255 (1978)].
[25] V.A. Kiselev, Fiz. Tverd. Tela (Leningrad) **21**, 1069 (1979) [Sov. Phys. Solid State **21**, 621 (1979)].
[26] V.A. Kiselev, Pis'ma Zh. Éksp. Teor. Fiz. **29**, 369 (1979) [JETP Lett. **29**, 369 (1979)].
[27] A.S. Batyrev, V.A. Kiselev, B.V. Novikov, and A.E. Cherednichenko, Pis'ma Zh. Éksp. Teor. Fiz. **39**, 436 (1984) [JETP Lett. **39**, 528 (1984)].
[28] B.V. Novikov, E.A. Ubushiev, and A.E. Cherednichenko, Fiz. Tverd. Tela (Leningrad) **27**, 1359 (1985) [Sov. Phys. Solid State **27**, 821 (1985)].
[29] V.A. Kiselev, B.V. Novikov, S.S. Utnasunov, and A.E. Cherednichenko, Fiz. Tverd. Tela (Leningrad) **28**, 2946 (1986) [Sov. Phys. Solid State **28**, 1655 (1986)].
[30] V.A. Kiselev, B.V. Novikov, A.E. Cherednichenko, and E.A. Ubushiev, Phys. Status Solidi B **133**, 573 (1986).
[31] V.A. Kiselev, B.V. Novikov, A.S. Batyrev, E.A. Ubushiev, and A.E. Cherednichenko, Phys. Status Solidi B **135**, 597 (1986).
[32] A.S. Batyrev, A.E. Cherednichenko, and V.A. Kiselev, Fiz. Tverd. Tela (Leningrad) **29**, 2126 (1987) [Sov. Phys. Solid State **29**, 1221 (1987)].
[33] F. Pérez-Rodríguez and P. Halevi, Phys. Rev. B **45**, 11 854 (1992).
[34] P. Halevi and F. Pérez-Rodríguez, Fiz. Nizk. Temp. **18**, 1135 (1992) [Sov. J. Low Temp. Phys. **18**, 795 (1992)].
[35] F. Pérez-Rodríguez and P. Halevi, Phys. Rev. B **48**, 2016 (1993).
[36] B. Flores-Desirena, F. Pérez-Rodríguez, and P. Halevi, Phys. Rev. B **50**, 5404 (1994).
[37] A.S. Batyrev, N.V. Karasenko, and A.V. Sel'kin, Fiz. Tverd. Tela (St. Petersburg) **35**, 3099 (1993) [Phys. Solid State **35**, 1525 (1993)].
[38] A. D'Andrea and R. Del Sole, Phys. Rev. B **38**, 1197 (1988).
[39] A. D'Andrea and R. Del Sole, Phys. Rev. B **25**, 3714 (1982).
[40] J. Lagois, Phys. Rev. B **23**, 5511 (1981).
[41] L. Schultheis and I. Balslev, Phys. Rev. B **28**, 2292 (1983).
[42] L. Schultheis and J. Lagois, Phys. Rev. B **29**, 6784 (1984).